Joining of Dissimilar Aluminum Alloys AA2024 and AA7075 by Friction Stir Welding: A Review

Ajay Kaushal, Sachindra Shankar, and Somnath Chattopadhyaya

1 Introduction

Aluminum 2024 alloy has high ratio of strength to weight but the major problem with 2024 is that it has poor corrosive resistance and on this ground it is sometime cladded with more zinc containing aluminum alloys, i.e., 7 series alloys. As these alloys contain high strength to weight ratio, aerospace industries have always looked for better welding technique for 2XXX alloys. There are various techniques available for joining dissimilar aluminum alloys as shown in Fig. 1.

Vijay et al. [1] performed TIG welding of Al2024 and Al6063 by changing three types of input parameters such as gas flow rate, current and root gap. It was reported that with the increase in root gap, gas flow rate and current the TS of the joint increases. Nasser [2] performed MIG welding for aluminum alloys 2024-T351 and 6061-T651 using argon as shielded gas and ER- 4043(AlSi5) as a filler metal. Maximum ultimate tensile strength and tensile strength of about 323 and 295 MPa was achieved respectively. Third homogenous method used for welding of dissimilar aluminum alloy is laser welding. Zang et al. [3] performed CO_2 laser welding of aluminum alloys 2024 and 7075 using different filler materials. Tensile strength of 339.5 and 308.6 MPa was reported when 2319 and 4043 were used as filler materials. Homogenous joining process used for joining dissimilar aluminum alloys of 2XXX and 7XXX series does not give sufficient strength because of higher susceptibility to hot cracking. For this reason solid-state welding processes are used for welding 2XXX and 7XXX series. Vaporizing foil actuated welding is quite similar to explosive welding with the difference in the driving force for weld formation. In this process, very fast electrical vaporization of thin foil takes place which results in the formation of very high pressure pulse that moves away thin flyer sheets to very high speed [4]. Highest ultimate tensile force was observed when the standoff distance was halved [5]. Second

A. Kaushal (✉) · S. Shankar · S. Chattopadhyaya
Department of Mechanical Engineering, IIT (ISM) Dhanbad, Dhanbad, Jharkhand, India

S. K. Natarajan et al. (eds.), *Recent Advances in Manufacturing, Automation, Design and Energy Technologies*, Lecture Notes in Mechanical Engineering,
https://doi.org/10.1007/978-981-16-4222-7_11

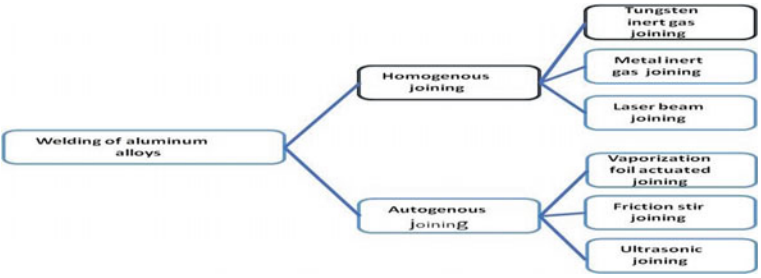

Fig. 1 Different processes used for joining of dissimilar aluminum alloys

solid-state welding process used is ultrasonic welding process wherein the plates to be welded are kept one over the other and the ultrasonic vibration were given to the top plate and due to friction between plates heat energy is produced and after obtaining sufficient heat the vibration are stopped and pressure is applied to form the weld [6]. FSW is the highly used process for welding AA2024 and AA7075 dissimilar alloys together. AA2024 and AA7075 alloys mainly finds its application in aerospace industries where it is required to have high strength at lower weight [7, 8]. FSW process is mainly used in welding of aluminum alloys as all the earlier process used are performed at high temperature leading to high susceptibility to hot cracking.

2 Process of FSW

FSW process can be subdivided into 4 phases which are shown in Fig. 2: plunging, dwelling, welding, dwelling and pulling out.

The last two phases, i.e., dwelling and pulling out are non productive process but they are only there to finalize the weld joint and hence cannot be avoided. In the

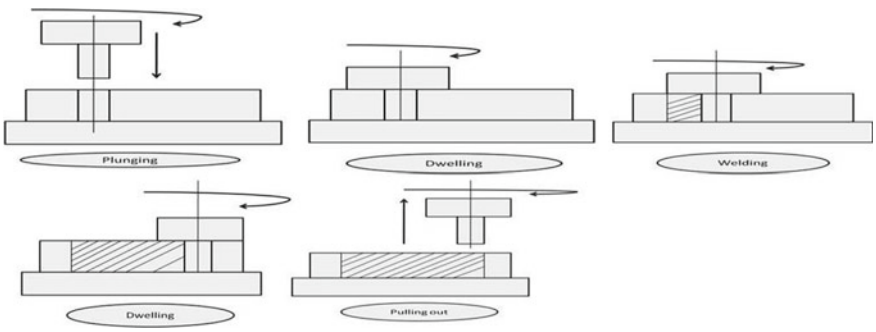

Fig. 2 Different phases of FSW

first phase, the tool is plunged into the workpiece and in order to reduce the vertical force in the z-direction a pre-technological hole can be made. After the rotating tool has been plunged into the workpieces it stays there for some time and this phase is called dwelling phase. During dwelling phase, there is velocity difference between stationary work pieces and rotating tool heat gets produced by the frictional forces. After producing sufficient heat between the tool and the workpiece third phase, i.e., welding phase starts wherein the tool is traveled along the weld center producing a joint between the base metals [9].

3 Parameters Effecting the Welded Joint

Figure 3 shows the parameter effecting FSW process. Heat generated in the course of FSW process is the main factor which controls the mechanical properties of the welded joint formed. Heat generated depends mainly upon the downward pressure or downward normal force acts on the tool and the rotational speed of shoulder and pin. Traveling velocity of the tool determine the rate of heat input and material flow around the tool nib. As the linear velocity (v) of the tool increases the heat rate reduces and at a particular location tool spends less time now which gives rise to smaller Stir Zone (SZ) [10]. The positioning of the material also influences the properties of the joint formed. To achieve better results (weld quality) in FSW process of dissimilar metals mainly harder material is put on the advancing side and softer material is put on the retreating side but in case of AA2024 and AA7075 the reverse shows better results [11, 12]. Khodir et al. [10] reported that maximum T.S of the welded joint was obtained when AA2024 (AA7075 is more hard when compared to AA2024) was put on the advancing side. The ratio (velocity ratio) of tool spinning speed and tool traveling speed also influences the welded joint. Devaraju et al. [13] reported that when the velocity ratio increase then microhardness also increases this happens because of more heat input causing softening of the material leading to more intense stirring of the soften metal in the WZ and this results in the grain refinement, ultimate tensile strength and yield strength also improves because of this grain refinement. Tool nib design used also effect the mechanical properties of the joint produced [13].

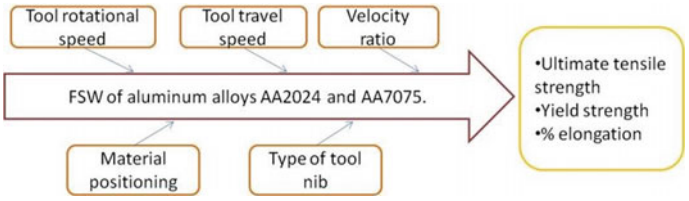

Fig. 3 Fish bone diagram representing the cause and its effect on the welded joint

4 Macrostructure

Figure 4 shows the macrostructure of the FSW welded dissimilar aluminum alloys AA2024 and AA7075 at different material positioning and linear speed. The 3 zone which are observed under optical microscope are (1) SZ or NZ, (2) TMAZ and (3) HAZ. Stir zone or nugget zone is the area surrounding the weld line where actually stirring of the base material occurs and due to this stirring or mixing the when the weld zone gets solidified onion ring like structure can be observed [10]. It is clear from Fig. 5 that on increasing the welding speed size of the stir zone decreases this happens because on increasing the linear velocity the heat concentration at a particular point will decrease leading to less softening of material which results in reduced stirring of the weld material in the nugget zone. TMAZ is around the NZ on both sides and this TMAZ is surrounded by HAZ. Outside the HAZ there is BM which is the unaffected region. The defects like kissing bond and tunnel defects were reported by Khodir et al. [10] when FSW was performed at high linear velocity keeping AA7075 on AS of the joint. Kissing bond is the descriptive term for two surfaces which are very close to each other but not so close that the majority of the surface irregularities gets deformed sufficiently and form metallic bonds. Depending upon the location and extent of the kissing bond defect the load bearing capacity and fatigue life of the component gets effected [14]. The tunneling defect occurs mainly due to lack of material flow and insufficient heat input [15].

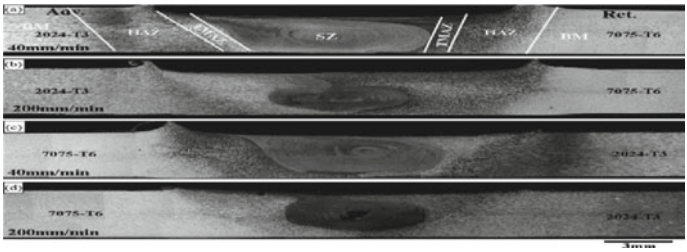

Fig. 4 Macrostructure of FSW dissimilar aluminum alloys AA2024 and AA7075 at different welding position and linear velocity [10]

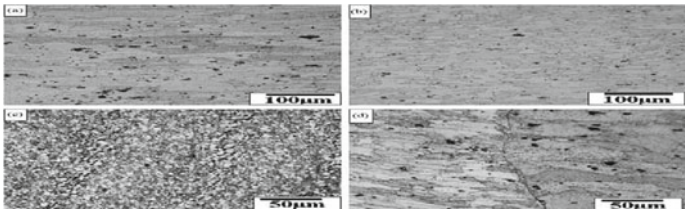

Fig. 5 Microstructure in base metal and stir zone, **a** base metal AA2024, **b** base metal AA7075, **c** onion rings, **d** kissing bond defect [10]

5 Microstructure

Figure 5a and b represents microstructure of the BM of AA2024 and AA7075 respectively. The micro-structural grains can be seen elongated in the direction of rolling along with the random distribution of the constituent particles. These random distributed particles are represented by black color in the microstructure and from figure it is also clear that the concentration of the constituent particles are more in the AA2024 side than on the AA7075 side.

Figure 5c represents microstructure of the onion rings in the stir zone when welding was performed keeping AA2024 on advancing side and at 1.2 mm/s [10]. In the microstructure bands of course and fine grains can be observed and the average sizes of these grains are 5.8 and 4.1 μm [10]. Figure 5d shows the kissing defect when the welding was performed keeping AA2024 on the retreating side, i.e., on the right side kissing crack and at tool travel speed of 3.3 mm/s. The kissing cracks are formed due to inadequate metal flow of the BM or improper acumen of tool nib at the weld root due to insufficient heat generation during the process.

Figure 6 shows the different zone observed in the optical microscope. Due to severe plastic deformation and higher temperature in the SZ at a space of 2 mm from the center of the weld on the AA2024 side fine equiaxed grains formed. In the stir zone of AA7075 side the grains become bigger in dimension and less equiaxed character was observed. In the TMAZ zone due to less heating (low temperature) no recrystallization occurs and so the deformed grains were observed in this region (Fig. 7). At an interval of 4 mm from the center of weld more parent metal grains are observed and this region coincides to HAZ wherein low micro-hardness was observed when compared to that of base metal [17]. Zhang et al. [18] performed FSW of similar and dissimilar AA2024 and AA7075 aluminum alloys of 5 mm thickness at varying speed of 600, 950, 1300, 1650 rpm. It was observed that the size of TMAZ is greater on RS side as compared AS and on increasing the tool rotational speed TMAZ size increases on both sides. Zhang et al. [19] performed quantitative analysis of the FSW AA2024 and AA7075 and it was observed that when the welding speed was reduced from 240 mm/min to 60 mm/min then the average grain size increases from 2.54 ±

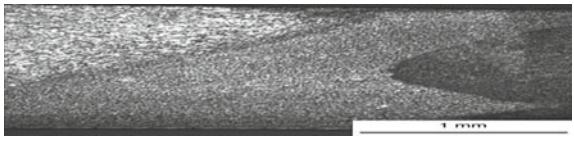

Fig. 6 Microstructure showing SZ, TMAZ and base metal [16]

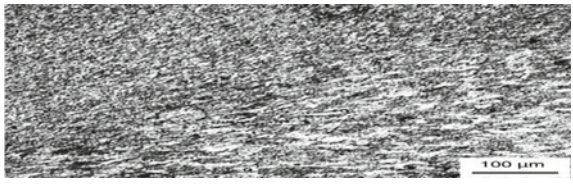

Fig. 7 Microstructure showing deformed grains in the TMAZ zone [16]

1.2 μm to 3.34 ± 1.8 μm this happens because the low tool traverse speed produces high thermal cycle in the NZ.

6 Mechanical Properties

6.1 Tensile Strength

Gowthaman et al. [11] performed the FSW of AA2024 and AA7075 using varying rotational speed and linear speed. The tool spinning speed was diverse in between 1000 to 1400 rpm and similarly the tool traverse speed was diverse in between 20 mm/min to 40 mm/min (Fig. 8). When tool was rotating at speed was 1000 rpm with travel speed was 20 mm/min the maximum tensile and Y.S of about 214.2 MPa and 191.8 MPa were observed. When the graph was plotted then a decrease in tensile strength was observed from 1000 rpm and $v = 20$ mm/min to 1200 rpm and $v = 30$ mm/min this is due to the development of fine strengthening precipitates and uniform equiaxed grains in the weld zone [11].

Srinivas et al. [20] reported that on increasing the velocity ratio, i.e., the ration of rotational speed of tool to its travel speed the U.T.S, Y.S and % Elongation increases (Fig. 9) because of increase in the heat generated which is entered into the weld but after a limit as this velocity ratio is increased then the strength of the weld decreases due to matrix softening wherein when the heat generation become more than a particular value then there is dissolution and/or coarsening of the strength giving precipitates in the aluminum matrix [20].

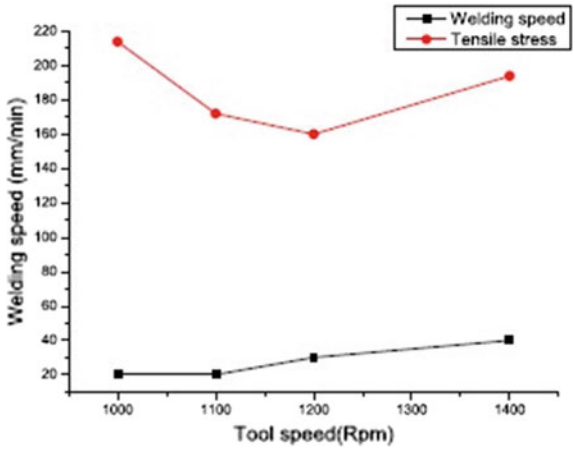

Fig. 8 Graph showing the variation in tensile strength with linear and rotational velocity [11]

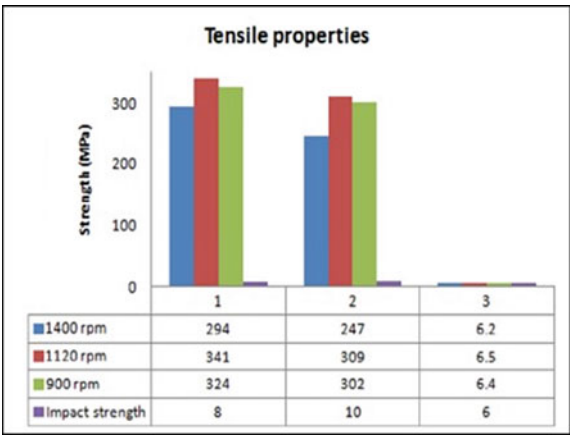

Fig. 9 Tensile property of the samples of dissimilar welded aluminum alloys at various velocity ratio [20]

6.2 *Micro-Hardness*

Figure 10 represents micro-hardness distribution of AA2024 and AA7075 at 40 and 200 mm/min. The rock bottom value of micro-hardness was noted in the HAZ on the AA2024 side this happens because in HAZ coarsening of precipitates lead to loss in the consistency with the matrix due to changing temperature [10]. On increasing the welding speed, the heat affected zone starts shifting toward the weld center, and this happens because of less heat interaction in the welding zone. The randomness of the hardness value in the stir zone is due to onion ring formation wherein bands of AA2024 (lower hardness) and AA7075 (higher hardness) are formed. Slightly decreased value of the hardness as compared to stir zone is noted in the TMAZ [10].

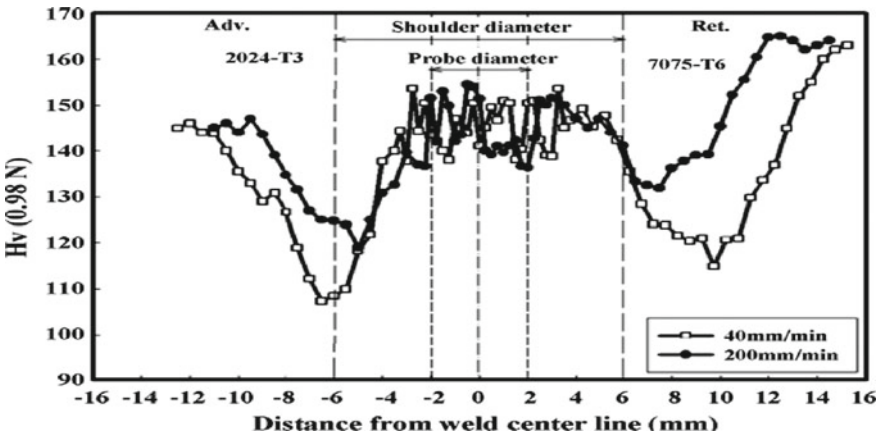

Fig. 10 Micro-hardness dessemination on the transversal section of the FSW joint at various tool travel speed [10]

7 Conclusion

From the FSW of AA2024 and AA7075 following conclusions can be drawn:

- The location of facture of all either similar or dissimilar joint coincides with the minimum hardness value in the particular joint.
- The harness value of both similar or dissimilar joint first increases and then decreases when moved along the weld thickness from top to bottom.
- Under the effect of high strain rate and quasistatic loading yield stress of both AA2024 and AA7075 decreases [21].

References

1. Vijay, S., Rajanarayanan, S., Ganeshan, G.N.: Analysis on mechanical properties of gas tungsten arc welded dissimilar aluminium alloy (Al2024 & Al6063). Mater. Today Proc. **21**, 384–391 (2020). https://doi.org/10.1016/j.matpr.2019.06.136
2. Al-Ramahi, N.J.N.: Mechanical properties of MIG joints for dissimilar aluminum alloys (2024–T351 and 6061–T651). Al-Khwarizmi Eng. J. **12**, 121–128 (2016)
3. Zhang, D., Zhao, Z., Gao, S., Zhao, H.: Research on CO_2 laser welding with filler wire of dissimilar high strength aluminum alloy 2024 and 7075. In: 2012 Symposium on Photonics Optoelectronics, SOPO 2012, p. 3 (2012). https://doi.org/10.1109/SOPO.2012.6270445
4. Hahn, M., Weddeling, C., Taber, G., Vivek, A., Daehn, G.S., Tekkaya, A.E.: Vaporizing foil actuator welding as a competing technology to magnetic pulse welding. J. Mater. Process. Technol. **230**, 8–20 (2016). https://doi.org/10.1016/j.jmatprotec.2015.11.010
5. Meng, Z., Wang, X., Guo, W., Hu, Z., Vivek, A., Hua, L., Daehn, G.S.: Joining performance and microstructure of the 2024/7075 aluminium alloys welded joints by vaporizing foil actuator welding. J. Wuhan Univ. Technol. Mater. Sci. Ed. **34**, 368–372 (2019). https://doi.org/10.1007/s11595-019-2061-7
6. Kumar, S., Wu, C.S., Padhy, G.K., Ding, W.: Application of ultrasonic vibrations in welding and metal processing: a status review. J. Manuf. Process. **26**, 295–322 (2017). https://doi.org/10.1016/j.jmapro.2017.02.027
7. Mishra, R.S., Ma, Z.Y.: Friction stir welding and processing. Mater. Sci. Eng. R Reports. **50**, 1–78 (2005). https://doi.org/10.1016/j.mser.2005.07.001
8. Meng, X., Huang, Y., Cao, J., Shen, J., dos Santos, J.F.: Recent progress on control strategies for inherent issues in friction stir welding. Prog. Mater. Sci. **115**, 100706 (2021). https://doi.org/10.1016/j.pmatsci.2020.100706
9. Durdanović, M.B., Mijajlović, M.M., Milčić, D.S., Stamenković, D.S.: Heat generation during friction stir welding process. Tribol. Ind. **31**, 8–14 (2009)
10. Khodir, S.A., Shibayanagi, T.: Friction stir welding of dissimilar AA2024 and AA7075 aluminum alloys, Mater. Sci. Eng. B Solid-State Mater. Adv. Technol. **148**, 82–87 (2008). https://doi.org/10.1016/j.mseb.2007.09.024
11. Gowthaman, P.S., Saravanan, B.A.: Determination of weldability study on mechanical properties of dissimilar Al-alloys using friction stir welding process. Mater. Today Proc. (2020). https://doi.org/10.1016/j.matpr.2020.08.599
12. Guo, J.F., Chen, H.C., Sun, C.N., Bi, G., Sun, Z., Wei, J.: Friction stir welding of dissimilar materials between AA6061 and AA7075 Al alloys effects of process parameters. Mater. Des. **56**, 185–192 (2014). https://doi.org/10.1016/j.matdes.2013.10.082
13. Devaraju, M., Manichandra, B., Jeshrun Shalem, M., Manzoor Hussain, M.: Impact on mechanical properties & metallographic of solid state welded 2024 & 7075 Al alloys dissimilar joint

by varying its parameters. Mater. Today Proc. **24**, 937–941 (2020). https://doi.org/10.1016/j.matpr.2020.04.405
14. Oosterkamp, A., Oosterkamp, L.D., Nordeide, A.: "Kissing bond" phenomena in solid-state welds of aluminum alloys. Weld. J. (Miami, Fla) **83**, 225-S (2004)
15. Al-Moussawi, M., Smith, A.J.: Defects in friction stir welding of steel. Metallogr. Microstruct. Anal. **7**, 194–202 (2018). https://doi.org/10.1007/s13632-018-0438-1
16. Cavaliere, P., Nobile, R., Panella, F.W., Squillace, A.: Mechanical and microstructural behaviour of 2024–7075 aluminium alloy sheets joined by friction stir welding. Int. J. Mach. Tools Manuf. **46**, 588–594 (2006). https://doi.org/10.1016/j.ijmachtools.2005.07.010
17. Muruganandam, D., Ravikumar, S., Das, S.L.: Mechanical and micro structural behavior of 2024–7075 aluminium alloy plates joined by friction stir welding. In: Proceedings of International Conference on Frontiers in Automobile and Mechanical Engineering-2010, FAME-2010, pp. 247–251 (2010). https://doi.org/10.1109/FAME.2010.5714835
18. Zhang, C., Huang, G., Cao, Y., Zhu, Y., Liu, Q.: On the microstructure and mechanical properties of similar and dissimilar AA7075 and AA2024 friction stir welding joints: effect of rotational speed. J. Manuf. Process. **37**, 470–487 (2019). https://doi.org/10.1016/j.jmapro.2018.12.014
19. Zhang, C., Huang, G., Liu, Q.: Quantitative analysis of grain structure and texture evolution of dissimilar AA2024/7075 joints manufactured by friction stir welding. Mater. Today Commun. **26**, 101920 (2020). https://doi.org/10.1016/j.mtcomm.2020.101920
20. Srinivas, B., Devaraju, A.: Investigation of velocity ratios on mechanical and microstructural characterization of friction stir welded dissimilar 2024 and 7075 aluminium alloy. Mater. Today Proc. **5**, 19250–19254 (2018). https://doi.org/10.1016/j.matpr.2018.06.282
21. Chao, Y.J., Wang, Y., Miller, K.W.: Effect of friction stir welding on dynamic properties of AA2024-T3 and AA7075-T7351. Weld. J. (Miami, Fla) **80**, 196–200 (2001)